

An analytical and numerical study of solar chimney use for room natural ventilation

Ramadan Bassiouny^{*}, Nader S.A. Koura

Department of Mechanical Power Engineering and Energy, Minia University, Minia 61111, Egypt

Received 17 May 2007; received in revised form 11 June 2007; accepted 19 June 2007

Abstract

The solar chimney concept used for improving room natural ventilation was analytically and numerically studied. The study considered some geometrical parameters such as chimney inlet size and width, which are believed to have a significant effect on space ventilation. The numerical analysis was intended to predict the flow pattern in the room as well as in the chimney. This would help optimizing design parameters. The results were compared with available published experimental and theoretical data. There was an acceptable trend match between the present analytical results and the published data for the room air change per hour, ACH. Further, it was noticed that the chimney width has a more significant effect on ACH compared to the chimney inlet size. The results showed that the absorber average temperature could be correlated to the intensity as: ($T_w = 3.51I^{0.461}$) with an accepted range of approximation error. In addition the average air exit velocity was found to vary with the intensity as ($v_{ex} = 0.013I^{0.4}$).

© 2007 Elsevier B.V. All rights reserved.

Keywords: Solar chimney; Natural ventilation; ACH; CFD

1. Introduction

Efficient air ventilation and thermal comfort are of great importance in rural areas and hot climate conditions. Ventilation is the intentional supply of fresh outdoor air to a space to dilute and remove indoor air contaminants. Ventilation, whether naturally or mechanically, is a very urgent need in many residential and industrial zones. Natural ventilation occurs due to two causes: aeromotive or wind driving force, or buoyancy driving force (stack effect) due to temperature difference between indoor and outdoor air temperatures. A significant temperature difference should be existed for the thermal driving force or stack effect to be appreciated. Use of solar energy can create such a large temperature difference, and hence improve the stack effect for space natural ventilation.

The solar chimney is an effective practical way to enhance space natural ventilation. In most tropical countries, where it is almost very difficult for the majority to have an air conditioner, people rely on natural ventilation, instead, to achieve comfort through opening windows. However, in some climates, where

the wind effect is not significant, just opening windows cannot effectively move the air inside the space to help diluting contaminants, odors, and satisfying the comfort feeling. This is due to the small pressure difference between the indoor and outdoor air. The solar chimney design and construction allow storing an amount of solar energy into a surface, then releasing this energy to an adjacent column of air raising its temperature, and accordingly it flows upward entraining an outdoor fresh air into the space. This will create an air breeze inside the space. The main driving force in moving the air upward in the chimney is the buoyancy force due to the absorbed energy.

Generally, solar energy with high intensity is available in the Middle East countries. Egypt in general and upper-Egypt in particular, has rich sunny and clear skies. These conditions encourage adopting such a concept to enhance building natural ventilation and save energy. Hence this was the motivation behind the present study.

2. Previous studies

The solar chimney is an attractive idea for many researchers in different fields. Some previous studies have been seen in the literature that investigates the use of solar chimney, with different configurations, in ventilation improvement. Some

^{*} Corresponding author. Tel.: +20 16 3916415; fax: +20 86 2346674.

E-mail address: ramadan9@yahoo.com (R. Bassiouny).

Nomenclature

A	area (m^2)
ACH	air change per hour (h^{-1})
b	chimney inlet size (m)
C_d	coefficient of discharge
C_p	specific heat ($\text{kJ}/(\text{kg } ^\circ\text{C})$)
d	chimney width (m)
g	gravitational acceleration (m/s^2)
Gr	Grashof number
h	heat transfer coefficient ($\text{W}/(\text{m}^2 \text{ } ^\circ\text{C})$)
H, H_w	room height and window height (m)
I	solar intensity (W/m^2)
k	thermal conductivity ($\text{W}/(\text{m } ^\circ\text{C})$)
L	chimney length (m)
Nu	Nusselt number
P	pressure (N/m^2)
Pr	Prandtl number
q	heat transfer (W)
Ra	Rayleigh number
T	temperature ($^\circ\text{C}$)
u, v	air velocity (m/s)
U	overall heat transfer coefficient ($\text{W}/(\text{m}^2 \text{ } ^\circ\text{C})$)
V	room volume (m^3)
W	room width (m)
x, y	coordinate system

Greek symbols

α	absorptivity
β	expansion factor
ε	emissivity (0.9 for glass and 0.95 for absorber wall)
ρ	density (kg/m^3)
σ	Stefan–Boltzmann constant ($5.67 \times 10^{-8} \text{ W}/(\text{m}^2 \text{ K}^4)$)
τ	transmittivity

Subscripts

a	ambient
c	chimney
cond	conduction
conv	convection
f	flow
g	glass
g–a	glass to air
l	loss
r	room
rw–g	radiative from wall to glass
rg–sky	radiative from glass to sky
w	wall
w–a	wall to air

researchers have been interested in analyzing the vertical chimney, while others have been studying the inclined chimney.

Bansal et al. [1] are the pioneers to study solar chimney configurations and performance. They developed a mathema-

tical model to study the effect of using solar chimneys on thermal-induced ventilation in buildings. A numerical solution of the proposed model revealed that the induced air flow ranged from 50 to 165 m^3/h for every square meter of the collector area and for solar radiation values of 100–1000 W/m^2 on the horizontal surface. Further, they found that the induced air flow depends on the geometry of the air collector, cross-section of the duct, and the performance parameters of the air-heating solar collector such as bottom and top loss coefficients and absorptance and transmittance of the collector plate glazing.

A theoretical and experimental study was carried out by Mathur et al. [2] to evaluate the possibility of making use of solar radiation to induce room ventilation in hot climates. The theoretical results of the proposed model were in a good agreement with the experimental ones. They found out that air flow increases linearly with the increase in solar radiation or the air gap between absorber and the glass cover.

Macias et al. [3] presented a practical approach to improve the passive night ventilation in social housing by applying the solar chimney concept. Instead of using fan forced ventilation, they used an accessible high thermal mass in building construction to collect solar energy during the afternoon in their concrete walls ($\sim 50^\circ\text{C}$). For every flat there was a separate chimney with a swinging flap at top, and while collecting energy the flap was closed. Then, during night when the ambient temperature drops to about 20°C the flaps at the top were opened generating a draft through flats, cooling down the thermal masses of the ceiling and walls.

Herreo and Heras-Celemin [4] proposed a mathematical model to evaluate the energy performance of a 2 m high solar chimney with a 0.24 m concrete wall as a thermal storage. Real weather data for the Mediterranean was used as initial conditions for the model. The concrete wall reached its higher temperature at 2 h later than the ambient temperature. Also, it maintained its temperature well after the beginning of the dark, inducing night natural ventilation. They recommended further studies to be pursued on the thermal inertia of solar chimneys.

An experimental study on a test cell resembling an actual room size was conducted by Chungloo and Limmeechockai [5]. They studied the effect of solar chimney and/or water spraying over a roof on natural ventilation. When the ambient temperature was 40°C , they achieved a maximum of 3.5°C reduction in temperature for the case of separate chimney, and a maximum of 6.2°C reduction in temperature for the combined effect of solar and water spraying. Also, they reported that the temperature difference between the inlet and outlet of the solar chimney tends to decrease during the period of high solar radiation and high ambient temperature. On the other hand, water spraying increases the temperature difference and consequently the air flow rate through the chimney. Finally, they recommended further studies to be carried out on the stack effect on natural ventilation with low rates of Reynolds number.

Mathur et al. [6] investigated the effect of using a solar chimney for enhancing natural ventilation. They found that there was a trade off between the absorber inclination and stack height. Experiments showed that the optimum absorber

inclination angle varies from 40° to 60° , depending on the latitude of the place. They compared the experimental results with the proposed mathematical model and found a good agreement in between.

An experimental investigation was carried out by Burek and Habeb [7] to study the effect of varying the solar intensity, resembled by an electric heater, from 200 to 100 W/m^2 , and the channel depth on mass flow rate through the channel. Temperatures and velocities were recorded and the mass flow rate was correlated to the heat input as $m \propto Q^{0.572}$ and to the channel depth as $m \propto S^{0.712}$.

Mathur et al. [8] studied the performance of some types of solar chimneys. First they investigated the performance of a cylindrical chimney when it is covered with a transparent cover and when it is uncovered. They found that the mass flow rate increases for the covered one. Then they studied the effect of inclination on a solar chimney, and concluded that an angel of 45° yields the highest rate of mass flow rate when compared with the vertical chimneys.

The previous available studies did not show detail information for air velocity distribution as air passes through the chimney, in addition to space inner-flow pattern. Also, there was no validation for the proposed correlations for the flow rate with both intensity and chimney depth. So, the present study focuses on studying the effect of the chimney inlet size measured from the room floor, air gap between the glass and absorber on flow pattern and air velocity variation through the chimney. It also aims at depicting air flow pattern under different operating conditions.

3. Mathematical analysis

The physical domain configuration considered in the present study is shown in Fig. 1. This domain is considered a 1 m wide \times 1 m height, assuming a 1 m depth. An overall energy balance on the chimney is considered. This balance includes the glass cover wall, the black absorber wall, and the air in between. Certainly, some postulations are assumed to enable solving the mathematical model, and as a result there will be some sort of error due to the approximated solution. Flow through chimney was considered laminar and under steady-state conditions. Energy exchange through glass, air, and absorber was treated as one-dimensional. Air inlet to the chimney was considered to have the same room air average temperature. Energy exchange between other walls in the room and the surrounding was neglected.

3.1. Energy balance over the glass wall

Applying the energy balance concept on the glass wall under the aforementioned assumptions yields the following: Energy due to incident radiation + re-radiated energy from the absorber = convective energy by the air in the chimney + total losses from the glass wall:

$$\alpha_g A_g I + h_{rw-g} A_w (T_w - T_g) = h_{conv,g-a} A_g (T_g - T_f) + \sum q_{loss}$$

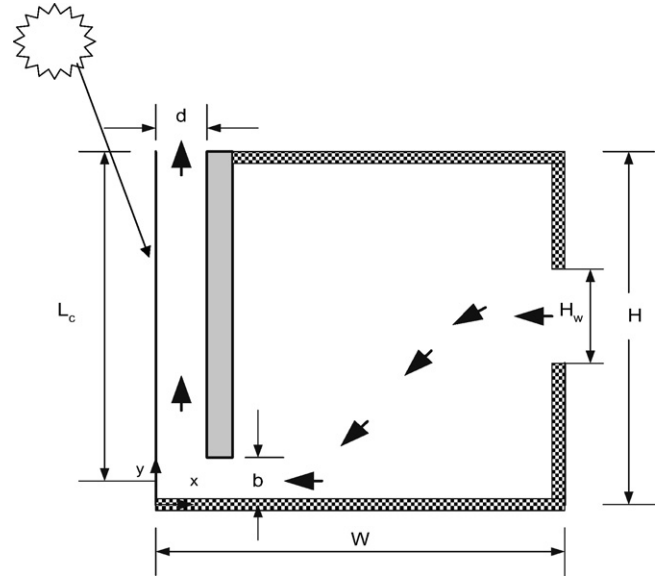


Fig. 1. A general schematic of the physical domain.

The last term in the right-hand side represents the losses from the glass wall to the surrounding by convection, radiation, and conduction:

$$\sum q_{loss} = q_{l-wind} + q_{l-sky} + q_{l-cond}$$

These losses can be summed up into

$$\sum q_{loss} = U_t A_g (T_g - T_a)$$

where U_t counts for the three heat transfer coefficients as

$$U_t = h_{wind} + h_{rg-sky} + h_{cond1}$$

So the above equations can be rewritten as

$$a_1 T_g + b_1 T_f + c_1 T_w = R_1 \quad (1)$$

where $a_1 = h_{rw-g} A_w + h_{conv} A_g + (h_{wind} + h_{rg-sky} + h_{cond1}) A_g$, $b_1 = -h_{conv,g-a} A_g$, $c_1 = -h_{rw-g} A_w$, and $R_1 = \alpha_g A_g I + (h_{wind} + h_{cond1}) A_g T_a + h_{rg-sky} A_g T_a$.

3.2. Energy balance over the flowing air

Similarly, applying the energy balance on the air column flowing through the chimney results in the following equation: Convective energy from the glass to the air + convective energy from the absorber to the air = convective energy by the air through the chimney.

This yield:

$$h_{conv,g-a} A_g (T_g - T_f) + h_{conv,w-a} A_w (T_w - T_f) = q_{conv}$$

where

$$q_{conv} = \dot{m} C_p (T_{fo} - T_{fi})$$

A mean temperature for the air flowing through the chimney can be calculated using a weighting factor between the inlet and outlet temperatures as

$$T_f = \omega T_{fo} + (1 - \omega) T_{fi}$$

Considering the air inlet to the chimney with a temperature is equal to the room average temperature T_r , and substituting in the above equation of q_{conv} gives the following equation:

$$q_{\text{conv}} = \dot{m} C_p \frac{T_f - T_r}{\omega}$$

where ω (mean temperature weighting factor) was found to be 0.74 in the literature [2]. Substitution and rearranging the above equation results in the following equation:

$$a_2 T_g + b_2 T_f + c_2 T_w = R_2 \quad (2)$$

where $a_2 = h_{\text{conv},g-a} A_g$, $b_2 = -h_{\text{conv},g-a} A_g + h_{\text{conv},w-a} A_w + (\dot{m} C_p / \omega)$, $c_2 = h_{\text{conv},w-a} A_w$, and $R_2 = -\dot{m} C_p T_r / \omega$.

3.3. Energy balance over the absorber wall

The absorber wall is the main trigger for the chimney theory of operation. The conservation of energy for this wall, as a part of the system, is as follows: Energy absorbed = re-radiated energy from the absorber to the glass + convective energy to the air in the chimney + conduction to the room:

$$\alpha_w \tau_g A_w I = h_{\text{rw-g}} A_w (T_w - T_g) + h_{\text{conv},w-a} A_w (T_w - T_f) + h_{\text{cond}2} A_w (T_w - T_r)$$

Rearranging the above equation gives

$$a_3 T_g + b_3 T_f + c_3 T_w = R_3 \quad (3)$$

where $a_3 = -h_{\text{rw-g}} A_w$, $b_3 = -h_{\text{conv},w-a} A_w$, $c_3 = h_{\text{rw-g}} A_w + h_{\text{conv},w-a} A_w + h_{\text{cond}2} A_w$, and $R_3 = \alpha_w \tau_g A_w I + h_{\text{cond}2} A_w T_r$. The above three equations, (1)–(3) are iteratively solved using the relaxation method. The temperatures of glass, absorber, and air in between are obtained. The flowing air properties are considered to vary with its temperature. Therefore, the properties are updated with the converged temperature values. The heat transfer coefficients listed in the above three equations can be calculated based on the Stefan–Boltzmann relation, Newton's cooling law, and Fourier law of conduction. These coefficients are as listed below:

$$h_{\text{rw-g}} = \frac{\sigma (T_w + T_g) (T_w^2 + T_g^2)}{((1 - \epsilon_g) / \epsilon_g) + ((1 - \epsilon_w) / \epsilon_w) + (1 / F_{w-g})}$$

where the shape factor, F_{w-g} is considered unity.

$$h_{\text{rg-s}} = \frac{\sigma \epsilon_g (T_g + T_{\text{sky}}) (T_g^2 + T_{\text{sky}}^2) (T_g - T_{\text{sky}})}{T_g - T_a}$$

Glass absorptivity was taken as 0.06, transmittivity as 0.84, and wall absorptivity as 0.95. The sky temperature and wind coefficient can be found in [9] as:

$$T_{\text{sky}} = 0.0552 T_a^{1.5} \quad \text{and} \quad h_{\text{wind}} = 2.8 + 3.0 V$$

The conductive heat transfer coefficients for the glass and absorber walls are

$$h_{\text{cond}1} = \frac{1}{(1/h_0) + (\Delta x_g / k_g)}, \quad h_{\text{cond}2} = \frac{1}{(1/h_i) + (\Delta x_{\text{ins}} / k_{\text{ins}})}$$

Air flowing in the chimney carries convective energies from the glass and absorber walls. So, the convective heat transfer coefficients between air and both walls are

$$h_{\text{conv},g-a} = \frac{Nu k_{f@T_g}}{L_g}, \quad h_{\text{conv},w-a} = \frac{Nu k_{f@T_w}}{L_w}$$

Once the converged temperatures are known, and the air properties are updated, the air flow rate can be calculated using the following relation [2,6]:

$$\dot{m} = \frac{C_d \rho_f A_0}{\sqrt{1 + (A_0^2 / A_i^2)}} \sqrt{2g L_c \left[\frac{T_f}{T_r} - 1 \right]}$$

The coefficient of discharge, C_d is defined as the ratio of the cross-section area at the vena-contracta to the actual opening area. Spencer [11] mentioned that the C_d value is almost constant at 0.61 for Re greater than 100, and less than 0.6 for Re less than 100. A value of 0.57 was chosen due to the sharp edge inlet.

In natural ventilation, it is much significant to know air exchange rate, the ratio of the air volume flow rate to the room volume. This expression is known as the air change per hour (ACH). This index is defined by ASHRAE as

$$\text{ACH} = \frac{\dot{V} \times 3600}{\text{room total volume}}$$

In this study, the room volume was considered 27 m³ to simulate an actual room size for the purpose of reasoning values and to compare with the published data in Ref. [2]. However, it should be noted that the room model volume could be used to obtain ACH.

Below are the correlations used to estimate the heat transfer coefficients between air flowing in the chimney and both glass wall and absorber wall [2]. The empirical relation for the Nusselt number is obtained from Ref. [10] for natural convection on vertical plates:

$$T_m = \frac{T_g + T_s}{2}$$

where T_s means a surface average temperature. It is equal to T_g when the system is the glass wall, and equal to T_w when the system is the absorber wall.

$$\beta = \frac{1}{T_m}, \quad \Delta T = T_s - T_f,$$

$$\mu_f = 1.846 \times 10^{-5} + 0.00472 \times 10^{-5} (T_m - 300),$$

$$k_f = 0.0263 + 0.000074 (T_m - 300),$$

$$C_p = 1007 + 0.004 (T_m - 300), \quad Pr = \frac{\mu C_p}{k_f},$$

$$Ra = Gr Pr = \left[\frac{g \beta \Delta T L_c^3}{\nu^2} \right] \frac{\mu C_p}{k_f},$$

$$Nu = 0.68 + \frac{0.67 Ra^{0.25}}{[1 + (0.492 / Pr)^{9/16}]^{4/9}}$$

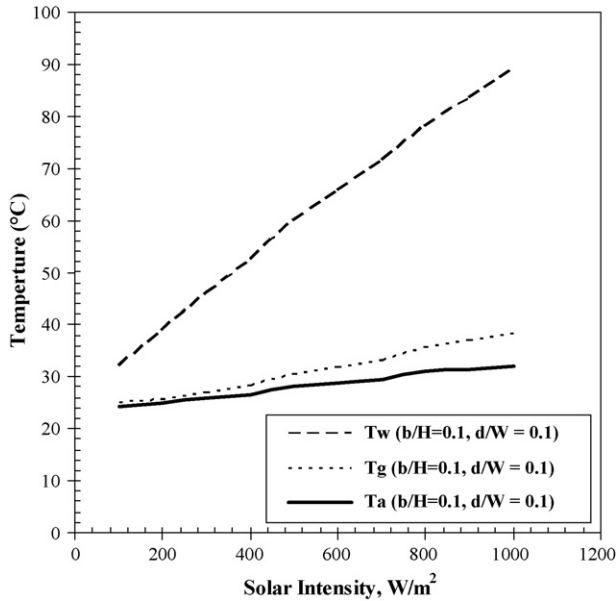


Fig. 2. Temperature variation of glass, wall, and air as a result of solar intensity variation.

4. Numerical analysis

The finite element method was used to predict flow pattern inside the space as a result of using a solar chimney. The main governing equations are considered as [10]:

$$\frac{\partial u}{\partial x} + \frac{\partial v}{\partial y} = 0, \quad u \frac{\partial u}{\partial x} + v \frac{\partial u}{\partial y} = g\beta(T - T_{\infty}) + \nu \frac{\partial^2 u}{\partial y^2},$$

and $\rho C_p \left(u \frac{\partial T}{\partial x} + v \frac{\partial T}{\partial y} \right) = k \frac{\partial^2 T}{\partial y^2}$

The momentum equation along with the energy equation was iterative and simultaneously solved. The flow was assumed to be incompressible, steady, and laminar. A quadrilateral element type was chosen over which a quadratic approximation of the dependent variable and the weighted function was assumed. The computational domain considered in this study is shown in Fig. 6. Mesh refinement is adopted in regions where sharp variation in the variable is expected, such as in the boundary layer region. A gradual mesh refinement was adopted

to prove a grid independent solution. The eventual total number of elements was 6510 elements.

5. Results and discussion

A FORTRAN computer program uses the relaxation iterative method to solve for wall, glass, and air average temperatures. These temperatures are the trigger for the whole analysis. Herein, the results are presented and discussed.

Solar energy transmission through the chimney will certainly create a significant temperature difference through the chimney. This difference is the driving force for chimney theory of operation. Fig. 2 shows the average temperature variation of glass wall, absorber wall, and air in between as a result of solar intensity variation. The figure indicates the significant temperature difference corresponding to solar intensity. Further, as intensity increases, there is almost a linear increase in all temperatures. The figure indicates that the maximum absorber temperature would increase by a factor of 2.25 when intensity increases by a factor of five. This is expected due to the nature of the absorber as a thermal storage medium. This absorbed energy increases the absorber temperature, the major part of this energy is consumed in accelerating the air through the chimney. Being mainly a transmittive medium, glass temperature is considerably low and close to that of air due to glass low absorptivity and exposure to convection from both sides. It can be concluded from the figure that the wall average temperature varies as $(3.51I^{0.461})$, while the glass average temperature varies as $(9.15I^{0.199})$.

The average exit velocity variation as a result of varying the inlet air size and chimney width is shown in Fig. 3. The figure shows that there is an optimum inlet size beyond which the air flow rate through the chimney would begin to decrease. In addition, increasing the chimney width beyond would relax the flow of kinetic energy, though the flow rate increases due to the effect of area increase.

The solar intensity is the motive force and its natural variation in the universe is significant for the chimney performance. Fig. 4a shows the effect of varying the chimney inlet size on the ACH at different solar intensities for a certain chimney width. This figure illustrates that the increase in the ACH as the solar intensity increase is approaching asymptotic

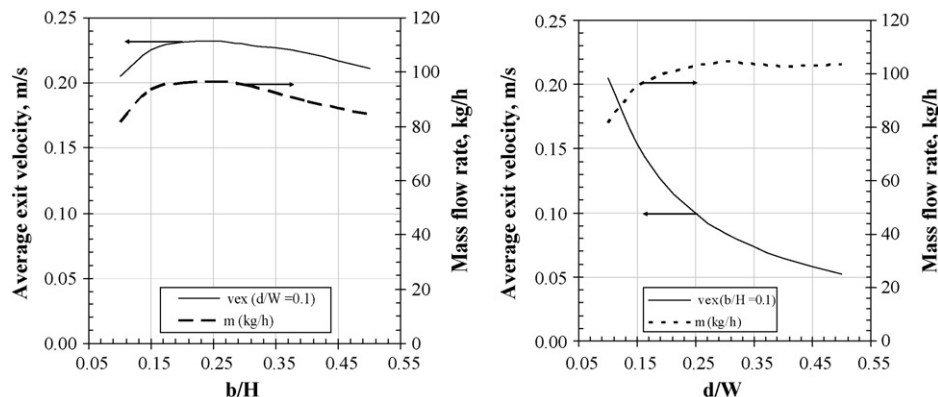


Fig. 3. Air average exit velocity and flow rate variation as a result of varying chimney width.

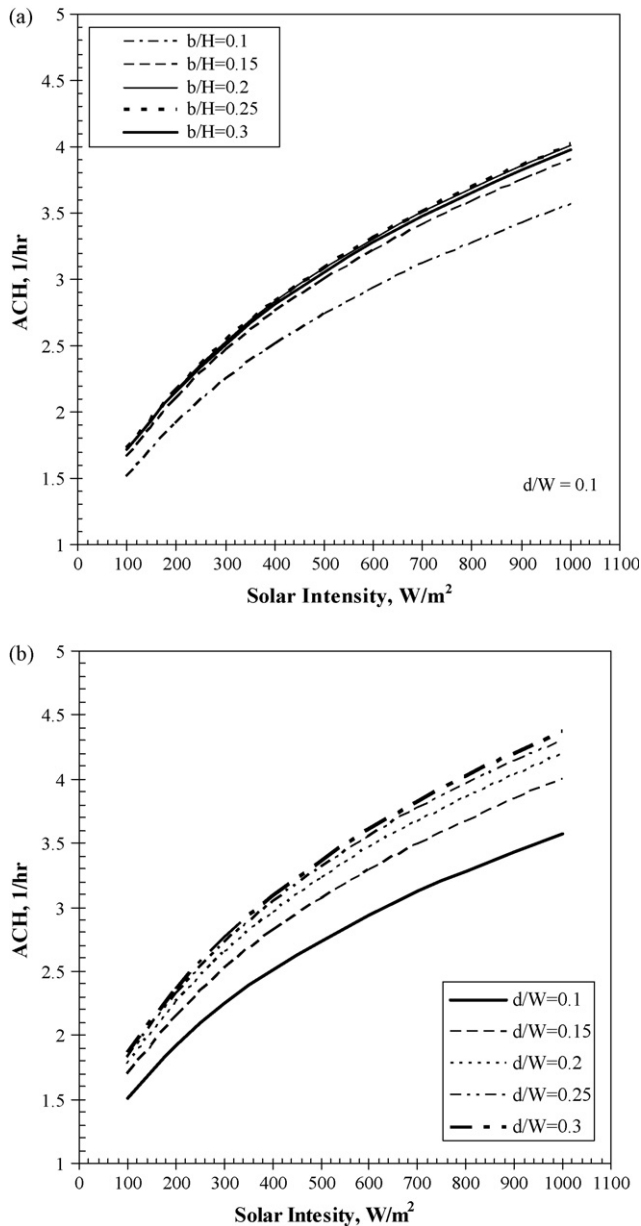


Fig. 4. ACH variation as a result of varying air inlet size (a) and chimney width (b).

trends. The figure also shows that there is a remarkable increase in the ACH at high solar intensities as the chimney inlet size increases up to almost 0.2 m, then any increase does not have a significant effect on ACH improvement. On the contrary, increasing the chimney inlet size beyond almost 0.25 m would tend to decrease the ACH. This could be attributed to the increase in air velocity at the inlet to the chimney at first, and then as the inlet size increases, the flow kinetic energy tends to relax and flow separation took place resulting in contracting the airsteam flowing up in the chimney. Thus, the exit velocity would reduce and consequently the flow rate.

Fig. 4b shows the effect of varying the chimney width on the ACH at a selected inlet air size and at different solar intensities. The figure illustrates a distinct improve in the ACH as the chimney width increases. This improvement would be

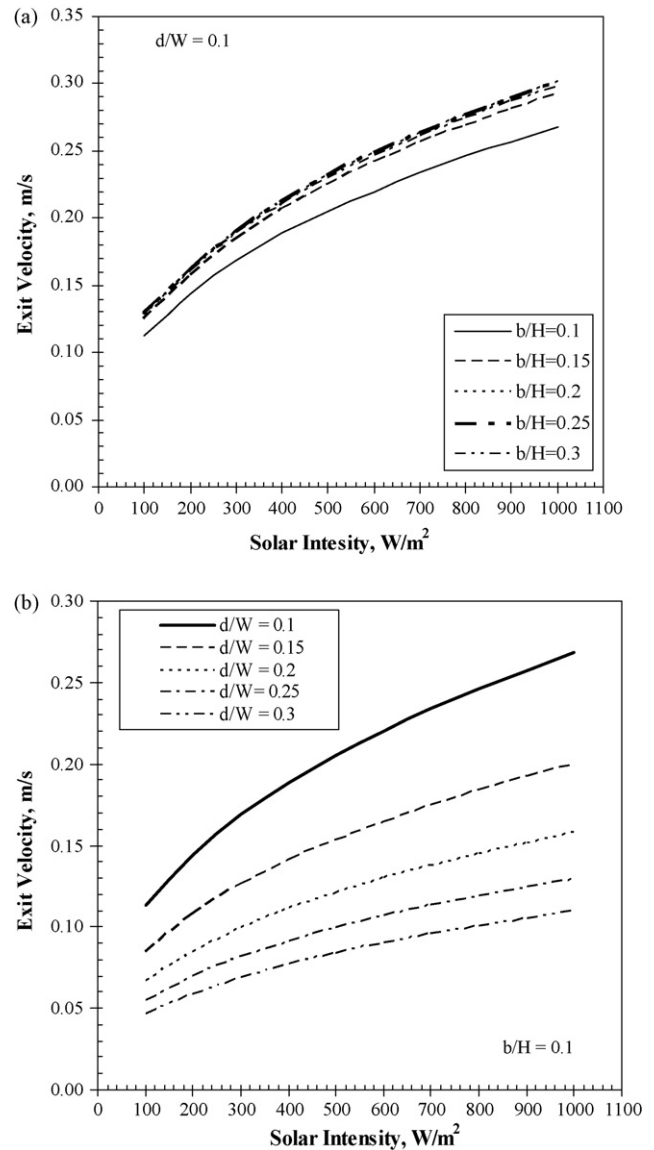


Fig. 5. Air exit velocity as a result of varying air inlet gap height (a) and chimney width (b).

insignificant beyond a chimney width of almost 0.25 m. Comparing Fig. 4a and b concludes that the chimney width has a more significant effect on the ACH than the inlet air size.

Fig. 5a shows the inlet air size effect on chimney average exit air velocity. This could help optimizing this size to reduce inlet losses and enhance ACH. For any intensity, an insignificant improvement in the exit velocity was noticed as the chimney inlet size increases. On the other side, Fig. 5b manifests that as the chimney width increases the exit velocity decreases due to the relaxation in the flow kinetic energy as chimney cross-section area expands. Also, it is clear from both figures that at high solar intensity, the variation in velocity is significant as the width varies from 0.1 to 0.3 m. This increase is due to the result of increasing the energy gained by the absorber causing the air in between the glass and absorber to highly accelerate (Fig. 6).

The inlet flow to the chimney is definitely affected by the discharge coefficient which is, in turn, dependent on the

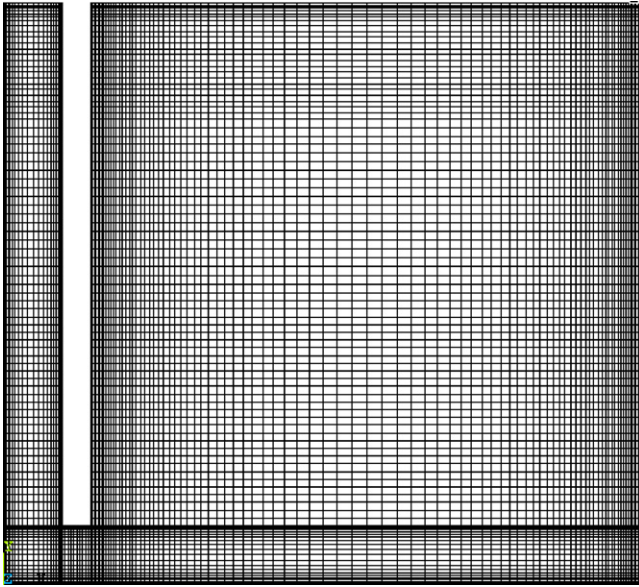


Fig. 6. Room and chimney grid configuration.

contracted area due to the sudden contraction in geometry to the main inlet area shape. Fig. 7 depicts an enlarged zoom on the flow velocity vectors beneath the absorber, where the flow is suddenly contracted. As shown, the sudden contraction increases the air velocity in this region, the vena-contracta effect. This creates flow separation just very close to the leading edge followed by a flow reattachment. This separation would add resistance on upward flow. Zones of secondary flow are illustrated by the figure.

Since the air gap between the absorber and the glass cover (chimney width) plays an important role in the ventilation rate, it is encouraged to closely depict the flow pattern as this gap varies. Fig. 8 shows the flow pattern and zones of separation as a result of varying the chimney width. Increasing the flow area width would increase the mass flow

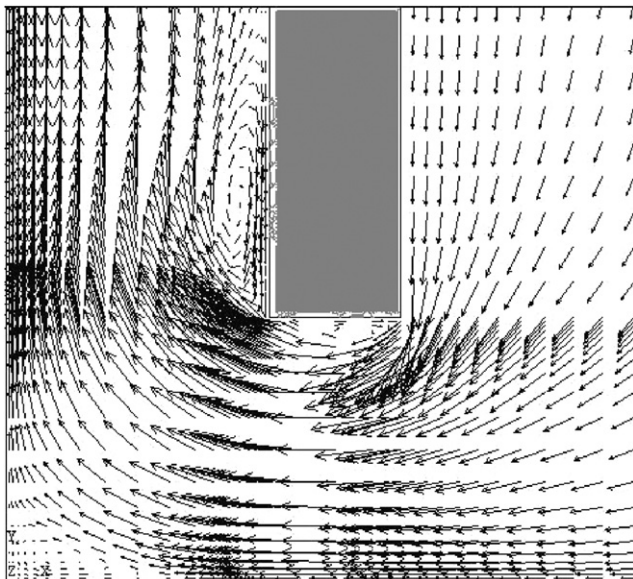
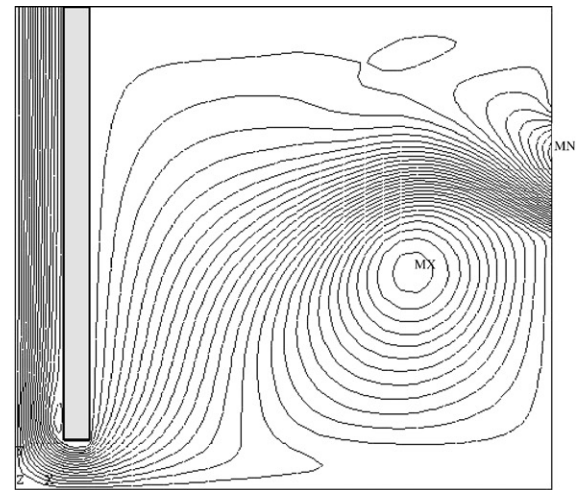
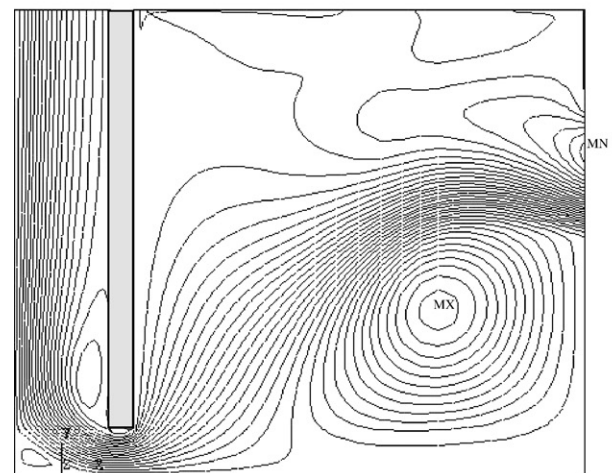


Fig. 7. An enlarged portion of the air flowing beneath the absorber wall.

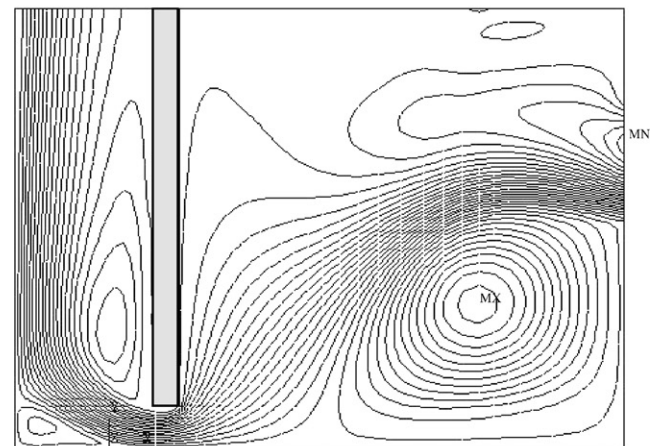
rate. Since the inlet area was kept constant, the inlet velocity would increase resulting in a noticeable flow separation region at the lower part of the chimney as shown in the figure. Increasing the chimney width allows the flow inside the space



(a) Width 0.1 m



(b) Width 0.2 m



(c) Width 0.3 m

Fig. 8. Stream function through the space and chimney for different chimney width at 300 W/m^2 solar intensity. (a) Width 0.1 m. (b) Width 0.2 m. (c) Width 0.3 m.

Table 1
Summary of some results for comparison with experimental and theoretical published data [2]

Absorber height (m)	Air inlet size b (m)	Chimney width (m)	Chimney height (m)	ACH at 300 W/m ²			ACH at 500 W/m ²			ACH at 700 W/m ²		
				Experimental [2]	Mathur et al. [2]	Present study	Experimental [2]	Mathur et al. [2]	Present study	Experimental [2]	Mathur et al. [2]	Present study
0.9	0.1	0.1	0.95	2	2.497	2.249	2.4	2.992	2.739	2.662	3.125	3.118
	0.1	0.2		2.8	2.949	2.650	2	3.392	3.227	3.73	3.879	3.671
	0.1	0.3		2.4	2.704	2.760	2.66	3.461	3.361	2.93	3.671	3.824
0.8	0.2	0.1	0.9	2.66	2.608	2.535	2.93	3.067	3.086	4	3.518	3.505
	0.2	0.2		4.53	3.633	3.480	4.26	4.049	4.233	3.73	4.688	4.806
	0.2	0.3		5.33	4.054	3.891	4.53	4.895	4.732	5.33	5.175	5.373
0.7	0.3	0.1	0.85	3.2	2.406	2.515	4	3.09	3.060	4.4	3.524	3.475
	0.3	0.2		4	3.619	3.705	5.2	4.205	4.503	5.2	4.942	5.112
	0.3	0.3		4.4	4.173	4.375	4.8	5.16	5.316	5.6	5.81	6.033

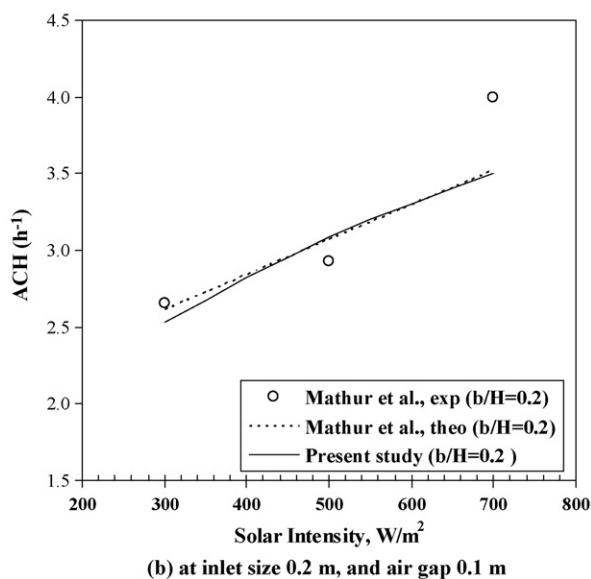
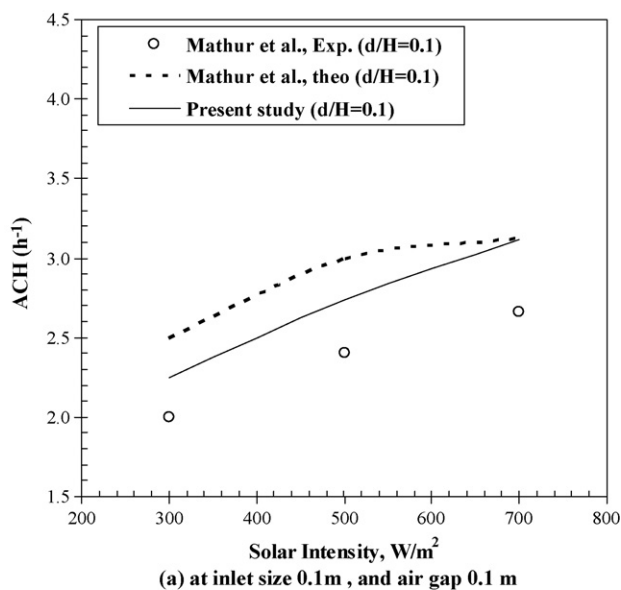


Fig. 9. Comparing with theoretical and experimental published data (a) at inlet size 0.1 m and air gap 0.1 m and (b) at inlet size 0.2 m and air gap 0.1 m.

to relax and fill in the occupied zone, which is very important in the ventilation field.

A comparison between the obtained results and the theoretical and experimental results of Mathur et al. [2] is shown in Fig. 9a and b. The present study considered a wide range of intensity variation from 100 to 1000 W/m², while only 300, 500, and 700 W/m² were considered in Ref. [2]. Selected results are compared with those obtained in Ref. [2]. A summary of these results for different configurations and solar intensities are listed in Table 1. There was a fluctuation of both theoretical results around the measured experimental data. However, this variation is accepted. The quantitative comparison showed a reasonable agreement between the results obtained during this study and the published results within the operating conditions they considered.

6. Conclusions

The present study shows that the chimney width has a very significant effect of flow rate and ACH compared to the inlet area size. The results showed that there is an optimum inlet size beyond which the room ACH would decrease. It can be concluded that increasing the inlet size three times only improved the ACH by almost 11%. However, increasing the chimney width by a factor of three improved the ACH by almost 25%, keeping the inlet size fixed. The numerical prediction of flow pattern showed the effect of absorber edge on flow separation and accordingly the energy dissipated. Chamfering the inlet sharp edge is expected to further improve the ventilation rate.

References

- [1] N.K. Bansal, R. Mathur, M.S. Bhandari, Solar chimney for enhanced stack ventilation, *Building and Environment* 28 (3) (1993) 373–377.
- [2] J. Mathur, N.K. Bansal, S. Mathur, M. Jain, Anupma, Experimental investigations on solar chimney for room ventilation, *Solar Energy* 80 (2006) 927–935.
- [3] M. Macias, A. Mateo, M. Schuler, E.M. Mitre, Application of night cooling concept to social housing design in dry hot climate, *Energy and Buildings* 38 (2006) 1104–1110.

- [4] J. Matrti-Herrero, M.R. Heras-Celemin, Dynamic physical model for a solar chimney, *Solar Energy* 81 (5) (2007) 614–622.
- [5] S. Chungloo, B. Limmeechockai, Application of passive cooling systems in the hot and humid climate: the case study of solar chimney and wetted roof in Thailand, *Building and Environment* 42 (9) (2007) 3341–3351.
- [6] J. Mathur, S. Mathur, Anupma, Summer-performance of inclined roof solar chimney for natural ventilation, *Energy and Buildings* 38 (2006) 1156–1163.
- [7] S.A.M. Burek, A. Habeb, Air flow and thermal efficiency in solar chimneys and trombe walls, *Energy and Buildings* 39 (2) (2007) 128–138.
- [8] J. Mathur, S. Anupma, Mathur, Experimental investigation on four different types of solar chimneys, *Advances in Energy Research* (2006) 151–156.
- [9] J.A. Duffie, W.A. Beckman, *Solar Energy Thermal Process*, John Wiley and Sons Inc., 1974.
- [10] J.P. Holman, *Heat Transfer*, McGraw-Hill Co., 1981.
- [11] S. Spencer, An experimental investigation of a solar chimney natural ventilation system, MSc Thesis, Concordia University, Montreal, Quebec, Canada, 2001.